Inorg. Chem. **2008**, *47*, 1020–1029

Synthesis, Structure, and Bonding of $Sc_4Mg_xCu_{15-x}Ga_{\sim 7.5}$ ($x = 0$, 0.5). Two Incommensurately Modulated Scandium Substitution Derivatives of Cubic $Mg_2Cu_6Ga_5$

Qisheng Lin,[†] Sven Lidin,[‡] and John D. Corbett*,[†]

Department of Chemistry, Iowa State University, Ames, Iowa 50010, Department of Chemistry, Stockholm University, Stockholm, Sweden 10691

Received September 19, 2007

The substitution of scandium for magnesium in $Mg_2Cu_6Ga_5$ (Mg_2Zn_{11}-type) yields an irrational superstructure phase that includes the refined compositions, $Sc_4Mg_{0.50(2)}Cu_{14.50(2)}Ga_{7.61(2)}$ and $Sc_4Cu_{14.76(2)}Ga_{7.51(2)}$. These crystallize in *Cmmm*, $a = \sim 8.31$ Å, $b = \sim 21.72$ Å, $c = \sim 8.30$ Å. The structures feature Sc_2 dimers, Cu_6 octahedra, a 3D CuGa ($Cu_{12}Ga_2$) framework, and arachno gallium-centered Cu_4Ga_6 icosahedra that are condensed into zigzag chains. The arrangement of these building blocks exhibits a topologic relationship to $Mg_2Cu_6Ga_5$. Further studies reveal that the quaternary compound exhibits incommensurate modulations along *a*, with $q = (0.694, 0, 0)$. Structure refinements with superspace group *Xmmm(a00)000* led to saw-tooth modulations for two fractional or mixed sites that avoid short Cu–Ga distances. Band structure analyses reveal that the Fermi surface and bonding are sensitive to the incommensurately modulated atoms.

Introduction

The growth in experience, insights, and knowledge regarding stoichiometry, crystal structure, electronic structure, and bonding relationships in polar intermetallic phases containing heavy triels (gallium, indium, and thallium) has been notable in recent years.[1−3] In particular, we have developed clearer ideas as to how to electronically tune compositions to special points near to where new quasicrystals[4] and, especially, their neighboring crystalline approximants[4,5] can be discovered. These are usually found in the region of about two valence electrons per atom ($e/a = 2.0$), neighbors of Hume−Rothery electron phases.[6,7] For example, the discovery of $Mg_2Cu_6Ga_5$ ($Pm\bar{3}$)[8] and a study of its electronic structure have enabled us to purposefully synthesize both the $Sc_3Mg_{0.17}Cu_{10.5}Ga_{7.25}$ 1/1 crystalline approximant (AC) and its corresponding quasicrystal (QC) via a new concept of tuning to a calculated pseudogap.[9] Since then, applications of pseudogap tuning to, specifically, Mg_2Zn_{11} and $Na_2Au_6In_5$ have also resulted the discoveries of both 1/1 and 2/1 ACs and QCs in the Sc−Mg−Zn and Ca−Au−In systems.[10,11]

Yet, this is not the end. The many other intermetallic phases with low valence electron counts per atom (e/a) are generally poorly studied or not yet known. For example, a recent study of $Ca_4Au_{10}In_3$ reveals its novel structure, a notably low e/a (1.59), the character of an electronic transformation that relates $Ca_4Au_{10}In_3$ to the isotypic Zr_7Ni_{10}, and possible electronic tunabilities.[12] In another example, a recent theoretical population analyses of the Laves-type $NaCd_2$ ($e/a = 1.67$) demonstrated the clear formation of interpenetrating polar cluster networks in this and related phases that coincides with the general structural description.[13]

* To whom correspondence should be addressed. E-mail: jcorbett@iastate.edu.
† Iowa State University.
‡ Stockholm University.

(1) Corbett, J. D. in *Chemistry, Structure, and Bonding of Zintl Phases and Ions*, Kauzlarich, S. M., Ed.; VCH Publishers: New York, 1996; p 139.
(2) Corbett, J. D. *Angew. Chem., Int. Ed.* **2000**, *39*, 670.
(3) Miller, G. J.; Lee, C.-S.; Choe, W. In *Inorganic Chemistry Highlights*; Meyer, G., Naumann, D., Wesemann, L., Eds.; Wiley-VCH: Weinheim, Germany, 2002; pp 21−53.
(4) Janot, C. *Quasicrystals: A Primer*, 2nd ed.; Oxford University Press: Oxford, U.K., 1994.
(5) Goldman, A. I.; Kelton, K. F. *Rev. Mod. Phys.* **1993**, *65*, 213.
(6) Hume-Rothery, W. *J. Inst. Metals* **1926**, *35*, 295.
(7) Mizutani, U. In *The Science of Complex Alloy Phases*; Massalski, T. B., Turchi, P. E. A., Eds.; TMS (The Minerals, Metals & Materials Society): Warrendale, Pennsylvania, 2005; pp 1−42.
(8) Lin, Q.; Corbett, J. D. *Inorg. Chem.* **2003**, *42*, 8762.
(9) Lin, Q.; Corbett, J. D. *J. Am. Chem. Soc.* **2005**, *127*, 12786.
(10) Lin, Q.; Corbett, J. D. *Philos. Mag.* **2006**, *86*, 607.
(11) Lin, Q.; Corbett, J. D. *J. Am. Chem. Soc.* **2007**, *129*, 6789.
(12) Lin, Q.; Corbett, J. D. *Inorg. Chem.* **2007**, *46*, 8722.
(13) Fredrickson, D. C.; Lee, S.; Hoffmann, R. *Angew. Chem., Int. Ed.* **2007**, *46*, 1958.

10.1021/ic701853c CCC: $40.75
Published on Web 12/29/2007

Table 1. Summary of Loaded Reactions, Reaction Conditions, Dominant Products, and EDX Results

ID	reaction	*e*/*a*	conditions[a]	main products[b]	EDX for dominant phase (Sc/Mg/Cu/Ga)
			$Sc_xMg_{6-x}Cu_{18}Ga_{15}$		
	x				
1	3.0	2.00	A	~50% 1/1 AC	
2	3.5	2.01	A	~60% 1/1 AC	
3	4.0	2.03	A	~80% new *Cmmm*	15.5(2)/0.1(1)/53.9(3)/30.5(4)
4	4.5	2.04	A	>90% 1/1 AC	
5	5.0	2.05	A	>90% 1/1 AC	
			$Sc_4Mg_yCu_{15-y}Ga_{7.52}$		
	y				
6	0.4	1.89	A	>95% new *Cmmm*	16.0(2)/1.4(4)/53.6(4)/29.0(4)
7	0	1.88	A	>95% new *Cmmm*	16.1(1)/0 / 52.0(3)/31.9(6)
8	0.4	1.89	Q	~80% 1/1 AC	
9	0	1.88	Q	~80% 1/1 AC	

[a] A: sample was reacted at 800 °C for 3 days, cooled to 570 °C at a rate of 10 °C/hr, and then slowly cooled to 400 °C at 2 °C/hr for crystal growth, followed by annealing at that temperature for 2 days; Q: sample was directly quenched from melts at 800 °C. [b] The 1/1 AC is the YCd_6-type $Sc_3Mg_{0.4}Cu_{10.5}Ga_{7.3}$ cubic phase; see also ref 9.

Nonpolar regions that separate the polar and nonpolar sites were also noted. Thus, explorations concerning intermetallics in low *e*/*a* regions, whether experimentally or theoretically, and regarding new or known phases, continue to tantalize our scientific imagination.

In the present article, we report a new network structure that also exhibits incommensurately modulated displacements for some atoms; a phase that has again been discovered during electronic tuning syntheses within the Sc−Mg−Cu−Ga system.[9] As such, it also exhibits close relationships to both the Sc−Mg−Cu−Ga 1/1 AC and the QC in both composition and structure as well as a superstructure of the parent $Mg_2Cu_6Ga_5$.

Experimental Section

Syntheses. The quaternary compound was encountered unexpectedly as the principal product (~80%) after an exploratory reaction of the Sc/Mg/Cu/Ga composition 4:2:18:15 that was designed to tune to the reported QC phase[9] (reaction 3, Table 1). The sample was equilibrated at 800 °C for 3 days, cooled to 570 °C at a rate of 10 °C/hr, and then slowly cooled to 400 °C at 2 °C/hr for crystal growth, and finally annealed at that temperature for 2 days.

Single-crystal diffraction revealed that the crystals occurred in space group *Cmmm* (No. 65), with $a = 8.312(2)$ Å, $b = 21.716(4)$ Å, and $c = 8.300$ (2) Å and refined to a composition of about $Sc_4Mg_{0.4}Cu_{14.6}Ga_{7.5}$. So, a reaction with that stoichiometry (reaction 6) (Table 1) and a parallel reaction without magnesium (reaction 7) were loaded and reacted under the same conditions. Powder diffraction analyses indicated that both resulted in high yields (>95%) in the new phase region (Figure S1 in the Supporting Information). The products have a metallic luster and well-faceted morphology, and they are inert in air at room temperature such that no change is observed in powder patterns, even after 24 months of exposure.

Two additional parallel reactions (reactions 8 and 9) were also run and quenched directly from melts at 800 °C (Table 1). Powder diffraction analyses revealed that both contained ~80% of the YCd_6-type 1/1 AC[9] plus unidentified phase(s), suggesting that a peritectoid reaction that converts the 1/1 AC and the unknown phase into the title phase occurs at a lower temperature. The new phase also exhibits a variable composition range according to the single crystal analyses of products 6 and 7; however, no attempt has been made to determine the maximum magnesium limit in it. A change of ±1.3% (= 0.5/39) in the total scandium loaded produces mainly the 1/1 AC phase (Table 1).

Powder X-ray Diffraction. Data acquisition was performed on a Huber 670 Guinier powder camera equipped with an area detector and monochromatic Cu Kα1 radiation ($\lambda = 1.540\,598$ Å). Powders were homogeneously dispersed on a Mylar film support with the aid of petrolatum. The step length was set at 0.005°, and the exposure time was 0.5 h. Figure S1 in the Supporting Information shows the XRD patterns for the products of reactions 3, 6, and 7 in Table 1, together with the simulated pattern calculated according to the single-crystal results for the quaternary compound.

SEM-EDX Analyses. The elemental compositions of several single crystals from each of the reactions 3, 6, and 7 were determined via semiquantitative energy-dispersive X-ray spectroscopy (EDX) on a JEOL 840A scanning electron microscope (SEM) equipped with an IXRF X-ray analyzer system and a Kevex Quantum light-element detector. To increase the accuracies, samples mounted in epoxy were carefully polished to avoid the influence of sample tilting. During measurements, samples were first scanned via backscattered electrons, from which phases with different compositions were clearly represented by their different darknesses. Then the detector was focused on each phase area to acquire its spectrum, with at least four readings being made for each phase. The average values (Table 1) were used to compare with the refined compositions from X-ray diffraction data.

X-ray Diffraction Studies. Single crystals were mounted on a Bruker APEX Platform CCD diffractometer equipped with graphite monochromatized Mo Kα ($\lambda = 0.71073$ Å) radiation for structure determination. Data sets were collected over one hemisphere with an acquisition time of 10 s per frame. Data integration and absorption and Lorentz polarization corrections were done by the *SAINT* and *SADABS* subprograms in the *SMART* software packages.[14] Structure determinations and refinements were performed with the *SHELXTL* version 6.1 subprogram.[15] Assignments of the space group *Cmmm* were made on the basis of the *mmm* Laue symmetry determined by the diffractometer, the systematic absences, and the mean $|E^2 - 1|$ values, and this was confirmed by the subsequent successful solutions and refinements of the structures.

The structure solution of a crystal from high yield quaternary reaction (reaction 6) is used as an example. Sixteen atoms were

(14) *SMART*; Bruker AXS, Inc.: Madison, WI, 1996.
(15) *SHELXTL*; Bruker AXS, Inc: Madison, WI, 2000.

first located by direct methods, 13 of which with suitable separations for Ga−Cu pairs and the other three for Sc−Cu/Ga pairs. Therefore, they were initially assigned to gallium and scandium, respectively. Subsequent isotropic least-square refinements proceeded smoothly and converged at R1 ~8.8%. Examination of the isotropic thermal parameters revealed that 8 of the 13 assigned gallium atoms were too heavy compared to the average of the other atoms (U_{iso}, 0.016 versus 0.008 Å^2), so they were tentatively assigned to copper in the subsequent refinements. Rechecking the displacement parameters after a few cycles showed that all of the atoms had reasonable isotropic values except for Cu7 (U_{eq} = 0.030 Å^2). This suggested a mixture with a lighter element or a partially occupied position. The latter was checked by allowing its occupancy to refine with others held at full occupancy. The refined value was 1.01(2), a full occupancy but still with a large U_{iso} (0.031 Å^2). Therefore, a Cu7/Mg admixture evidently accounts for the large isotropic parameter and was so assigned. (In the following, Cu7 identifies this site for convenience.) At this stage, examination of the difference Fourier map revealed a weakly diffracting position (1/4, 1/4, 0) with an intensity of about 13.4 e/Å^3 and a distance of 2.09 Å from Cu7. Assignments of either gallium or copper to this position did not change a lot in terms of occupancy and U_{iso} values (40% and 0.091 Å^2 for gallium versus 42% and 0.087 Å^2 for copper). However, the assignment of this position to Ga6 gave a better agreement between refined and experimental compositions according to EDX analyses (Table 1) and was more reasonable in terms of these atoms' distinctive structural roles and functionalities as well. Noteworthily, reversal of all of the copper and gallium sites in the refinements puts U_{iso} for all of the gallium (except Ga6) in the range of 0.014−0.020 e/Å,^{2} obviously too large compared with those for scantium, 0.0081−0.0096 e/Å,^{2} whereas those for copper (except Cu7), 0.0007−0.0068 e/Å,^{2} are relatively too small. In addition, assignments of copper/gallium admixtures to all of the normal copper and gallium positions result in either unstable refinements or deviations of occupancies from unity that remain within 3σ. The crystallographic discernment between copper and gallium is impressive, yet the same result has been repeatedly observed in other intermetallic phases, for example, in $Li_{13}Cu_6Ga_{21}$,[16] $Na_{34}Cd_6Cu_7Ga_{92}$,[17] $SrCu_2Ga$,[18] $Mg_2Cu_6Ga_5$,[8] and $Mg_{35}Cu_{24}Ga_{53}$.[19] Copper and gallium are easily distinguished in terms of their structural functionalities and coordination environments in this and other cases.

The final anisotropic least-squares refinement for sample 6, with a secondary extinction correction, converged at R1 = 2.72%, wR2 = 6.91%, and GOF = 1.069 for 90 variables and 1042 independent reflections. The maximum and minimum residual peaks in the final difference Fourier map were 1.14 and −1.37 e/Å.^{3} The refined composition is $Sc_4Mg_{0.50(2)}Cu_{14.50(2)}Ga_{7.61(2)}$ (Z = 4), or normalized, $Sc_{15.03}Mg_{1.88(8)}Cu_{54.49(8)}Ga_{28.60(8)}$, consistent with the EDX data, $Sc_{16.0(2)}Mg_{1.4(4)}Cu_{53.6(4)}Ga_{29.0(4)}$. Very similar situations were encountered during the refinement of a crystal from reaction 7, except that occupancies for unmixed Cu7 and Ga6 sites were ~76 and 51%, respectively. The final refinement converged at R1 = 2.99%, wR2 = 6.49%, and GOF = 1.108 for 89 variables and 1041 independent reflections. The maximum and minimum residual peaks in the final difference Fourier map were 1.13 and −1.91 e/Å.^{3} The refined composition is $Sc_4Cu_{14.76(2)}Ga_{7.51(2)}$, or normalized, $Sc_{15.03}Cu_{54.49(8)}Ga_{28.60(8)}$, reasonably consistent with the EDX data, $Sc_{16.1(1)}Cu_{52.0(3)}Ga_{31.9(6)}$. In this case, the equivalent to the mixed Cu7/Mg site in (reaction 6) refined as 76(2)% copper alone, which is reasonable inasmuch as there is no magnesium in this sample. Summaries of crystal data and refinement for the crystal from reaction 6 are given in Table 2. The refined positional parameters and equivalent isotropic displacement parameters are listed in Table 3. The anisotropic displacement parameters (Table S1 in the Supporting Information) and the cif for reaction 6 product are given in the Supporting Information, together with all of the crystallographic data (Tables S2−S4 in the Supporting Information) and cif for crystal 7.

Table 2. Crystal Data and Structure Refinement Parameters for $Sc_4Mg_{0.50(2)}Cu_{14.50(2)}Ga_{7.61(2)}$

space group, Z	*Cmmm*, 4
fw (g/cm^3)	1643.8
unit cell (Å)	
a	8.311(2)
b	21.719(4)
c	8.300(2)
V (Å^3)/d_c (Mg/m^3)	1498.2(5)/7.29
abs. coeff. (mm^{-1})	35.15
reflns collected/R_{int}	4725/0.0305
obs. indep./res./params	1042/0/90
R1/wR2 [$I > 2\sigma(I)$]	0.0272/0.0691
(all data)	0.0300/0.0706
res. peak and hole (e/Å^3)	1.14 and −1.37

The foregoing results normally signal reasonable structure solutions. The only indication of a problem is that the anisotropic displacement parameters (ADP) of Ga6 are very abnormal ($U_{11}/U_{22}/U_{33}$ > 140:1:1), as also shown by the observed electron densities mapped in Figure 1. In addition, somewhat larger U_{ij} values (<7:1) in certain directions are also found for Cu3, Cu4, Cu6, and Cu7. The reason must relate to their environments inasmuch as very similar pathologies appear for both structures (Table S1 versus Table S4 in the Supporting Information) and are implicit in the final incommensurate analyses as well.

Considering the special cell parameters' relationship ($a \approx c$), the abnormal ADPs, and the partial occupancies of Ga6, it was necessary to check whether alternative symmetries or cells existed or not. Therefore, datasets for several crystals from reaction 6 were collected by either SMART CCD or STOE IPDS II[20] instruments with longer exposure times. This time, all of the datasets showed additional reflections that could not be indexed with space group *Cmmm*, and $a = \sim 8.31$ Å, $b = \sim 21.72$ Å, $c = \sim 8.30$ Å. For example, an image frame from the former dataset, in part a of Figure 2 , shows that nearly all of the reflections are indexed, as shown by the boxes, circles, and crosses (which mean that the marked reflection is within the scan range of the current, the preceding, and the subsequent frames, respectively). However, there are two unindexed reflections in this image, A and B. Through a movable crosshair, indices of about (2.7, 2.0, −3.5) and (2.7, −2.0, −3.5) are indicated for A and B, respectively. This indicates a possible incommensurate modulation vector $q \approx (0.7, 0, 0.5)$. (An alternate treatment of the extra reflections as arising from the 3 × 1 × 2 superstructure of a normal crystal gave only poor refinements.) Actually, evidently incommensurate reflections were also seen in the *h0l* zone image constructed from the STOE IPDS datasets (part b of Figure 2).

According to the STOE IPDS data, incommensurate reflections were also found in *h2l*, *h4l*, *h6l*... zone photos, but not in *h1l*, *h3l*... zones in *Cmmm* symmetry; and the modulation vector was refined from all such reflections as (0.694, 0.002, 0.499). For simplicity,

(16) Tillard-Charbonnel, M.; Belin, C. *J. Solid State Chem.* **1991**, *90*, 270.
(17) Chahine, A.; Tillard-Charbonnel, M.; Belin, C. *Z. Kristallogr.* **1994**, *209*, 542.
(18) Fornasini, M. L.; Merlo, F. *J. Less-Common Met.* **1988**, *142*, 289.
(19) Lin, Q.; Corbett, J. D. *Inorg. Chem.* **2005**, *44*, 512.
(20) *STOE WinXPOW, STOE & Cie Gmbh*, verson 2.10; Hilpertst: Darmstadt, Germany, 2004.

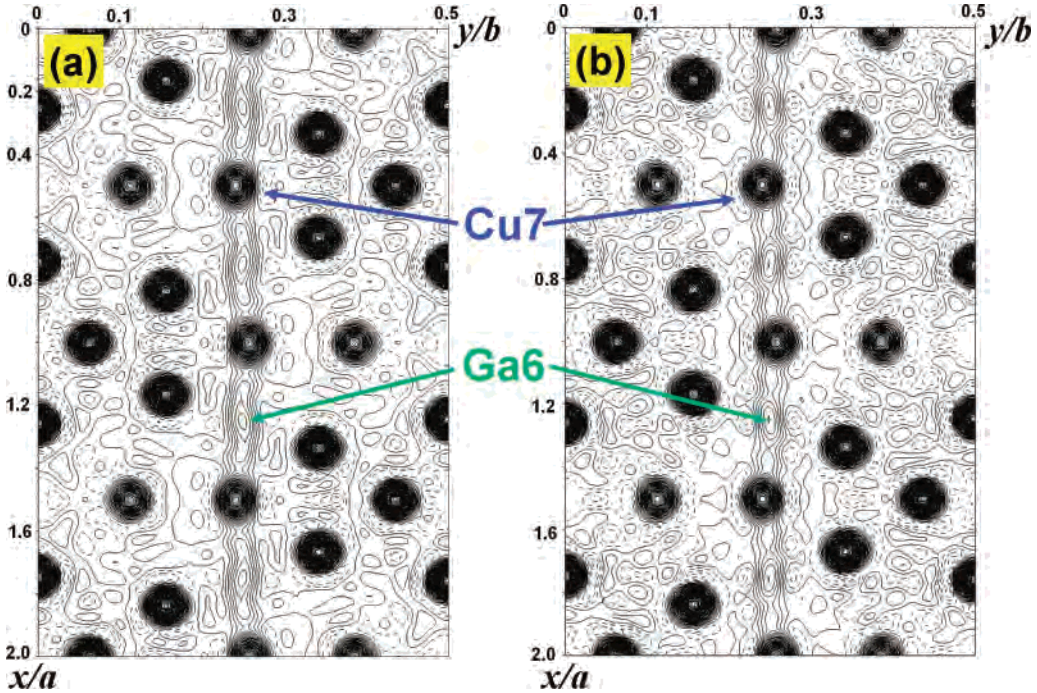

Figure 1. Projections of the observed Fourier map along the *c* direction, showing electron densities at Cu7/(Mg) and Ga6 positions in (a) $Sc_4Mg_{0.5}Cu_{14.5}Ga_{7.6}$ and (b) $Sc_4Cu_{14.8}Ga_{7.5}$. The plots are drawn at a contour level of 1 e/Å.[3] Solid and dashed lines denote positive and negative contours, respectively.

Table 3. Atomic Coordinates and Equivalent Isotropic Displacement Parameters for $Sc_4Mg_{0.50(2)}Cu_{14.50(2)}Ga_{7.61(2)}$ (Reaction 6)

atom	Wyck.	symmetry	x	y	z	U_{eq}(Å^2)	Occ. ≠ 100%
Cu1	16*r*	*1*	0.15898(8)	0.30661(3)	0.23436(8)	0.010(1)	
Cu2	16*r*	*1*	0.22331(8)	0.07959(3)	0.22368(8)	0.011(1)	
Cu3	8*p*	*..m*	0.1653(1)	0.15655(5)	0	0.017(1)	
Cu4	4*l*	*mm2*	0	1/2	0.1866(2)	0.012(1)	
Cu5	4*k*	*mm2*	0	0	0.2626(2)	0.015(1)	
Cu6	4*i*	*m2m*	0	0.06228(7)	0	0.016(1)	
Cu7/Mg	4*i*	*m2m*	0	0.2592(1)	0	0.018(1)	0.50/0.50(2)
Cu8	4*g*	*2mm*	0.2572(2)	0	0	0.012(1)	
Ga1	8*q*	*..m*	0.2461(1)	0.13293(4)	1/2	0.014(1)	
Ga2	8*n*	*m..*	0	0.40487(4)	0.3481(1)	0.011(1)	
Ga3	4*j*	*m2m*	1/2	0.42853(6)	1/2	0.013(1)	
Ga4	4*j*	*m2m*	0	0.30209(6)	1/2	0.014(1)	
Ga5	4*f*	*..2/m*	1/4	1/4	1/2	0.008(1)	
Ga6	4*e*	*..2/m*	1/4	1/4	0	0.60(5)	0.61(2)
Sc1	8*n*	*m..*	0	0.18491(7)	0.2961(2)	0.009(1)	
Sc2	4*i*	*m2m*	0	0.3871(1)	0	0.011(1)	
Sc3	4*h*	*2mm*	0.2983(3)	0	1/2	0.011(1)	

we used a doubled unit cell, that is, $a \times b \times 2c$, and $q = (0.694, 0, 0)$ to describe the structure in the superspace determination. Systematic absence analyses revealed the following extinctions: $hklm$, $h + k = 2n$, $l + m = 2n$ and $h + k + l + m = 2n$. The choice of setting yields an unconventional centering *X* with the components (1/2 1/2 0 0), (0 0 1/2 1/2), and (1/2 1/2 1/2 1/2), in which the first vector comes from the experimental observation, the second, from the doubling of the *c* axis, and the last, the sum of the former two components. Because no extinction conditions compatible with s-glides could be identified, the superspace group could be determined to be *Xmmm(α00)000*.[21]

The atomic coordinates of the 3D structure were transformed into the (3 + 1)*D* space group *Xmmm(a00)000* with the aid of the program *JANA2006*.[22] Subsequent isotropic refinements on both main and satellite reflections converged at R1 = 7.79%, wR2 = 12.56%. Then, first-order positional modulation waves were applied to all of the atoms, through which refinements improved to R1 = 5.41%, wR2 = 8.45% for the main reflections and R1 = 27.14%, wR2 = 35.43% for the first-order satellites. At this stage, examination of the x1−x4 sections through the atomic domains of Cu7 and Ga6 suggested that both exhibited saw-tooth-like modulation waves, and they were so assigned in subsequent isotropic least-squares refinements. These converged at R1 = 4.44%, wR2 = 6.22% for the main reflections and R1 = 22.9%, wR2 = 31.0% for the first-order satellite reflections. Table 4 summarizes the superspace refinement results, whereas the atomic positions, displacements, and other structural parameters are deposited in the Supporting Information (cif).

The atomic domains in the x4 direction show that Ga6 and Cu7 have the strongest modulation effects, followed by Cu3, Cu6, Cu4, and Ga3, whereas the remainder have negligible modulation waves. The modulations closely parallel the ADPs in the average structure

(21) Janssen, T.; Janner, A.; Looijenga-Vos, A.; de Wolff, P. M. *International Tables for Crystallography*; Kluwer Academic Publishers: Dordrecht, The Netherlands, 1995; Vol. C, Chapter 9.8.
(22) Petříček, V.; Dušek, M.; Palatinus, L. *JANA2006*; Institute of Physics: Praha, Czech Republic.

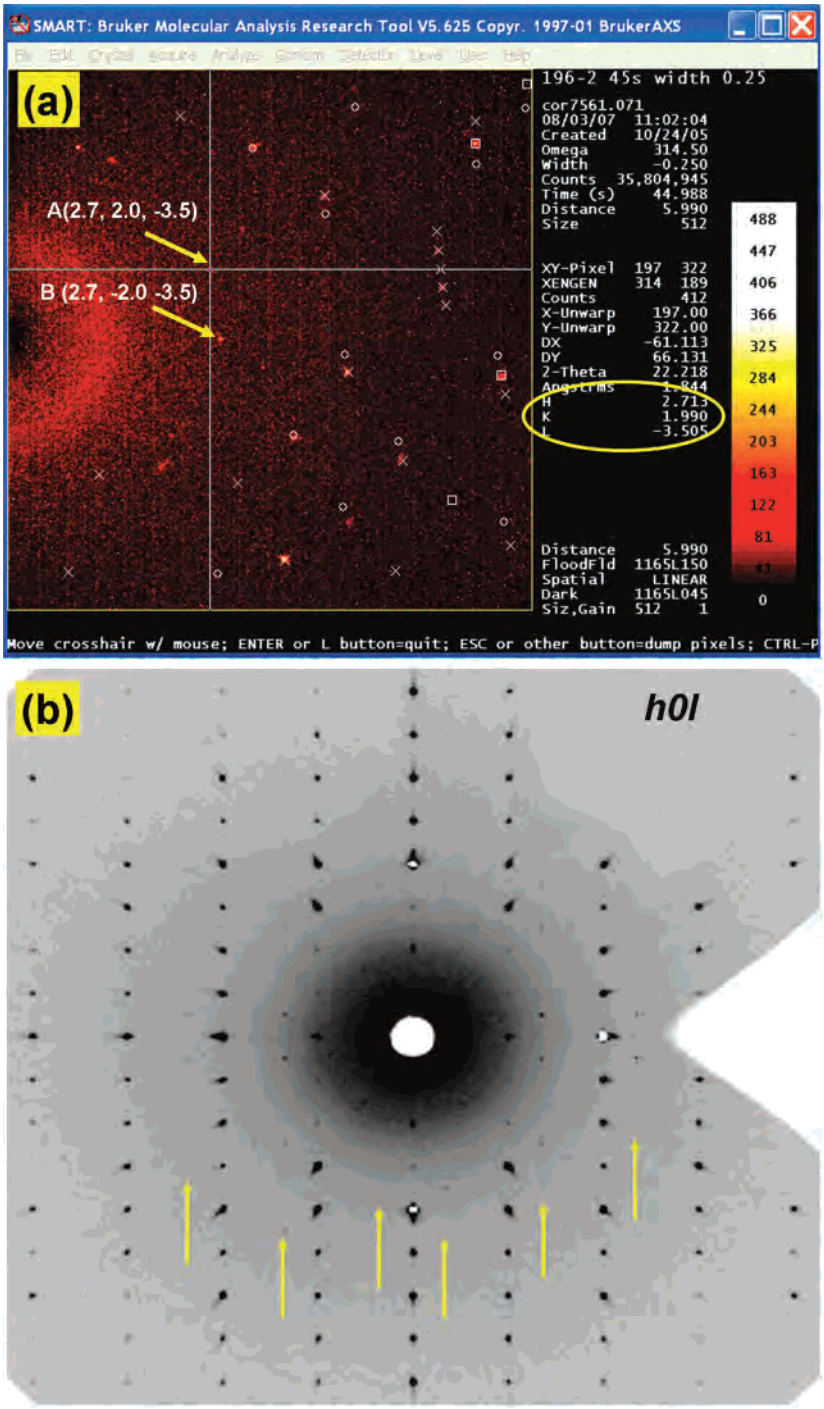

Figure 2. (a) Selected *SMART* CCD image frame from crystal $Sc_4Mg_{0.5}Cu_{14.5}Ga_{7.6}$ obtained at an exposure time of 45 s per frame, showing unindexed reflections with *Cmmm* symmetry. Two of the unindexed reflections are marked as A and B, with their corresponding *hkl* values. The circled *hkl* on the right side correspond to A, at the crosshairs. Boxes, circles, and crosses denote that the marked reflections are within the scan range of the current, the preceding, and the subsequent frames, respectively. (b) A reciprocal space view of the [*h0l*] zone of a dataset collected by STOE IPDS II with an exposure of 3 min/frame. Rows of incommensurate reflections are evident, as guided by arrows.

(Tables S1 and S4 in the Supporting Information). Moreover, the R1 and wR2 values of the first-order satellite reflections become quite large (43.1 and 57.4%) if the smaller positional modulation contributions for all but Ga6 and Cu7 are removed.

Note that the highest residual peak/hole densities (~11.8/−13.1 e/Å^3) are mainly a consequence of the inadequacy of the saw-tooth function, the artificial effects of least-squares refinements, and, of course, the limited data quality. The first effect is evident in both observed and difference Fourier maps (Figure S2 in the Supporting Information). Although the residual peaks could be decreased to ~7.2 e/Å^3 by adding, for example, ADP modulations for Ga6 and removing the saw-tooth function of Cu7, the difference maps did not justify this as a feasible structural model. The R values and residual peaks can be decreased more by adding, for example, second order positional modulation waves, anharmonic ADPs, and temperature modulations; however, these results are not straightforward in terms of refinements. The reason is that ~71.9% of the overall possible reflections are unobserved ($I < 3\sigma(I)$), and of those, 94.4% come from the satellite reflections. This is also the reason why the R values for the satellite reflections are very large (Table

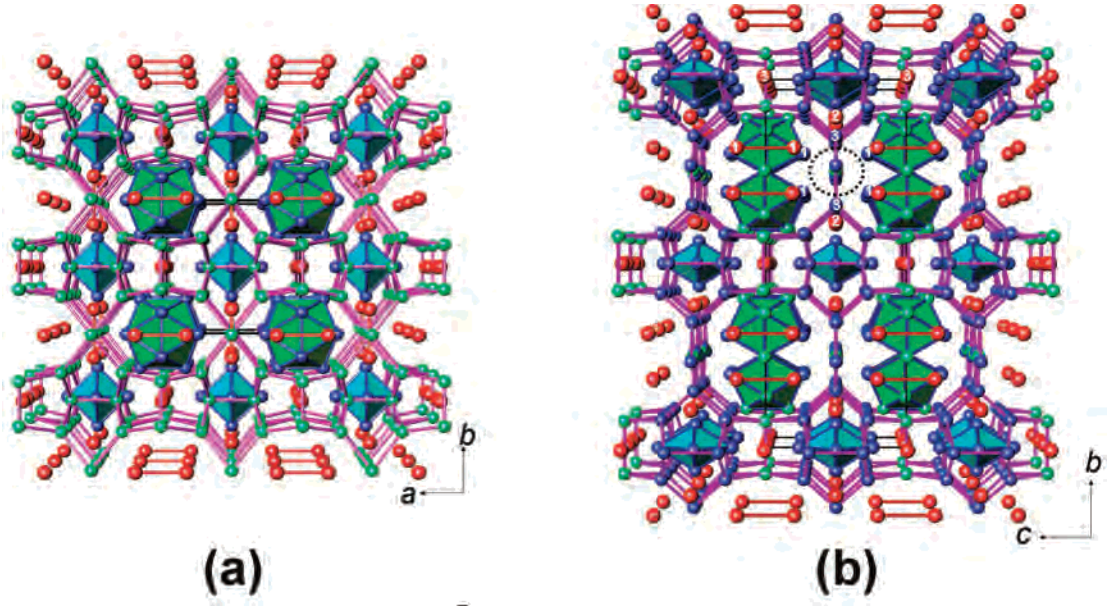

Figure 3. Perspective views of (a) cubic $Mg_2Cu_6Ga_5$ ($Pm\bar{3}$) and (b) orthorhombic $Sc_4Mg_xCu_{15-x}Ga_{\sim 7.5}$ (*Cmmm*), showing their topological structural similarities. The former contains Mg_2 dimers (red), Cu_6 octahedra (blue polyhedra), Ga@Cu_{12} icosahedra (green), and a 3D Ga_{14} framework (purple bonds). Structure (b), as a comparison, contains Sc_2 dimers (red), Cu_6 octahedra (dark blue), zigzag chains of Ga4-centered Cu_4Ga_6 arachno icosahedra (green) along *a*, and a 3D Cu(7)Ga(6)($Cu_{12}Ga_2$) open framework (purple bonds). This framework can also be viewed as 2D Cu_6@$Cu_{12}Ga_2$ layers bridged by Cu7 (or Cu7/Mg in the quaternary phase) and Ga6 atoms (dashed circled). Numbers are marked for selected atoms as listed in Table 3. Red spheres represent electropositive magnesium in (a) and scandium in (b); green, gallium; blue, copper (including Cu7/Mg). The same holds for following figures. Details about the building blocks in (b) are given in Figure 4.

Table 4. Incommensurate Structure Refinements of $Sc_4Mg_{0.50(2)}Cu_{14.50(2)}Ga_{7.61(2)}$

space group	*Xmmm*(*a*00)000, $q = (0.694, 0, 0)$
unit cell (Å)	
a	8.311(2)
b	21.719 (4)
c	16.600 (4)
data/res./params (overall)	5117/0/87
R_{obs} (overall) [$I > 3\sigma(I)$]	R1 = 0.0833, wR2 = 0.0704
R_{all} (overall)	R1 = 0.2467, wR2 = 0.0789
Obs./all (main reflns)	919/1124
R (main)	R1 = 0.0444, wR2 = 0.0622
Obs./all (first satellite refl.)	388/1957
R (first satellite)	R1 = 0.2288, wR2 = 0.3100
Obs./all (second satellite refl.)	132/2036
R (second satellite)	R1 = 0.6616, wR2 = 0.8041

4). Inasmuch as a long exposure dataset (5 min/frame) from the STOE IPDS II obviously did not improve the quality of the solution, further endeavors to justify a structure solution from these samples through laboratory X-ray diffractometer means were judged to clearly not be worth the time required. The same situation possibly holds for the ternary compound, as estimated from the average structural refinement results (Figure S1 in the Supporting Information).

Electronic Structure Calculations. Band structure calculations were performed for the average structure model by means of the self-consistent tight-binding linear-muffin-tin-orbital method in the local density and atomic sphere (ASA) approximations, within the framework of the DFT method.[23−26] As noted, the refined structures exhibit mixed Cu7/Mg and partially occupied Ga6 positions as major parts of the incommensurate structure. Therefore, the Ga6 atom was omitted in the calculations, and the Cu7/Mg sites were replaced by copper, which resulted in a formula of $Sc_4Cu_{15}Ga_7$. The ASA radii were calculated automatically, and no empty spheres were inserted with a maximum overlap restriction of 16%. All of the WS radii calculated are reasonable: 2.56−2.73 Å for gallium, 2.61−2.81 Å for copper, and 3.28−3.62 Å for scandium. The band structure was sampled with 24 × 24 × 24 *k* points in the irreducible wedge of the Brillouin zone. For bond analyses, the crystal orbital Hamiltonian population (COHP) method was used.[27] COHP data represent the energy contributions for all of the electronic states of selected bonds through partitioning the band structure energy in terms of the respective orbital pair contributions.

Results and Discussion

Phase Stability and Relationships to $Mg_2Cu_6Ga_5$ and Sc−Mg−Cu−Ga 1/1 AC. As implied in the experimental section, scandium substitutions in $Mg_2Cu_6Ga_5$ result in not only the $Sc_3Mg_{0.2}Cu_{10.5}Ga_{\sim 7.3}$ 1/1 AC and its corresponding *i*-QC phase[9] but also the title phase. The close relationships among these phases are in part shown by their similar chemical compositions. The ratio of electropositive to electronegative components in the title phase, $Sc_4Mg_xCu_{15-x}Ga_{\sim 7.5}$, lies within a range of 1:5.58 (4:22.3, $x = 0$) and 1:5.63 (4:22.5, $x = 0.5$) within its stoichiometry range, very close to those of $Mg_2Cu_6Ga_5$ (1: 5.50), the 1/1 AC (1: 5.97), and the Sc−Mg−Cu−Ga QC phase (1:5.67). More chemical aspects to this substitution process are also evident and will be considered after the structural analyses are described.

Structurally, the beginning and final relationships are also manifested in the cell parameters: $a_o \approx c_o \approx a_c$, $b_o \approx \tau^2 \times$

(23) Anderson, O. K.; Jepsen, O. *Phys. Rev. Lett.* **1984**, *53*, 2571.
(24) Jepsen, O.; Snob, M. *Linearized Band Structure Methods in Electronic Band-Structure and its Applications*, *Springer Lecture Note*; Springer-Verlag: Berlin, Germany, 1987.
(25) Shriver, H. L. *The LMTO Method*; Springer-Verlag: Berlin, Germany, 1984.
(26) Tank, R.; Jepsen, O.; Burkhardt, A.; Andersen, O. K. *TB-LMTO-ASA Program*, version 4.7; Max-Planck-Institut für Festkörperforschung: Stuttgart, Germany, 1994.
(27) Dronskowski, R.; Blöch, P. *J. Phys. Chem.* **1993**, *97*, 8617.

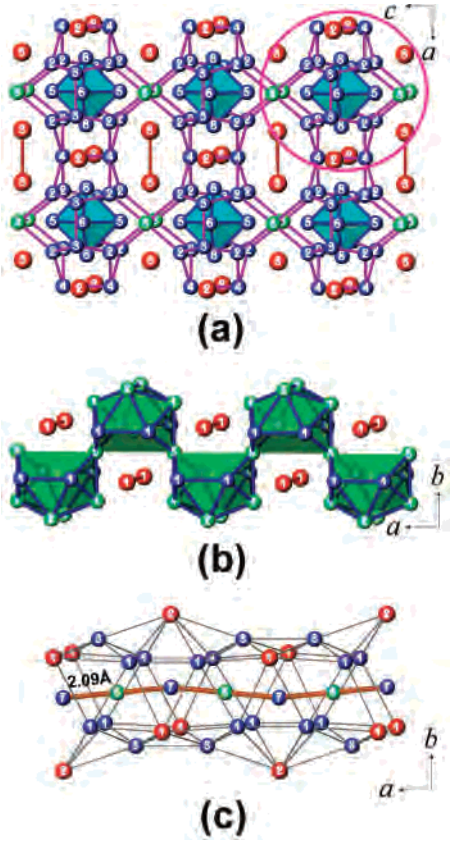

Figure 4. (a) Off-[010] projection of a single 2D $Cu_6@Cu_{12}Ga_2$ layer, in which one repeating unit is circled. (b) A zigzag chain of Ga4-centered Cu_4Ga_6 arachno icosahedra (green polyhedra) in $Sc_4Mg_xCu_{15-x}Ga_{\sim 7.5}$. Each arachno icosahedron adjoins a Sc1−Sc1 dimer, which forms a complete heteratomic icosahedron. Each Ga5 atom is also a center of another heteratomic icosahedron that contains two Sc1−Sc1 dimers, four Cu1, two Ga1, and two Ga4 atoms (see text). (c) Environments of Cu7 and Ga6 bridging atoms, which are incommensurately modulated in saw-tooth manner to form modulated chains along *a*.

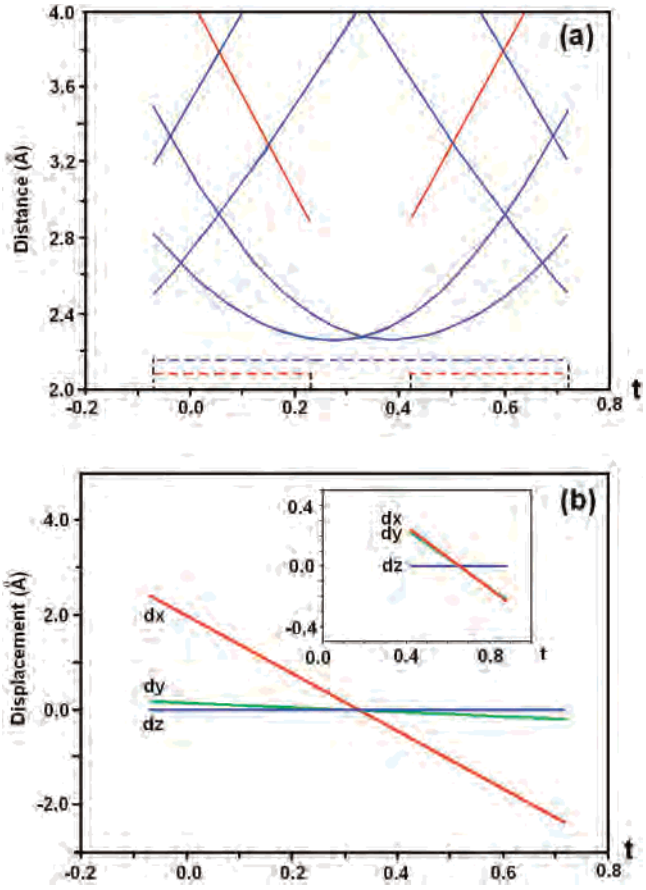

Figure 5. (a) Pairs of bond distances for Ga6−Cu3 (blue) and Ga6−Cu7/Mg (red). Dotted lines represent the mean bond distances in a 3D structure refinement. (b) The positional displacements of Ga6 (and Cu7/Mg, inset) in the three axial directions in terms of the internal t coordinates, which are the projections of $x4$ onto the A_4 axis along R_3 direction in $(3 + 1)D$ space.

a_c, in which the subscripts "o" and "c" denote the title orthorhombic and the primitive cubic $Mg_2Cu_6Ga_5$ phases, respectively, and $\tau = 1.618$ is the golden mean. Accordingly, the title phase is a $1 \times \tau^2 \times 1$ irrational superstructure of $Mg_2Cu_6Ga_5$. Inasmuch as $b_o \approx \tau \times a_{1/1} = a_{2/1}$, this phase can also be viewed as a 1D 2/1 AC.[28] In the following, we will discuss their detailed structural relationships.

Crystal Structure and Incommensurate Modulation. Being a closely related superstructure of $Mg_2Cu_6Ga_5$, the title compound certainly retains some features of its parent. Therefore, it is useful to review the structure motif of $Mg_2Cu_6Ga_5$ ($Z = 3$). As described before,[8] it can be conveniently written as $Mg_{2 \times 3}(Cu_6)(Ga@Cu_{12})Ga_{14}$, meaning that its structure, in part a of Figure 3, consists of four parts: Mg_2 dimers (red), Cu_6 octahedra (blue), $Ga@Cu_{12}$ icosahedra (green), and a Ga_{14} network (purple). The last exhibits a 3D open framework with large tunnels along *c* and small tunnels along *a* and *b*, in which the respective green $Ga@Cu_{12}$ icosahedra and the red Mg_2 dimers reside. In contrast, the blue Cu_6 octahedra are located in Ga_{14} cages. Therefore, the framework can be alternatively described as a 3D condensation of $Cu_6@Ga_{14}$ networking units through six shared Ga−Ga edges.

Part b of Figure 3 (drawn on the same scale) shows the superstructure of the title compound, in which a modified version of the former 3D open framework now has enlarged tunnels along *a* and *c* through the insertion of Cu7 and Ga6 bridging atoms. (The last are the atomic sites that are particularly incommensurate.) The large tunnels along *a* are filled with zigzag chains of Ga4-centered Cu_4Ga_6 arachno icosahedra (green polyhedra), and the small tunnels along *c*, by Sc2 atoms. Note that in $Mg_2Cu_6Ga_5$, all of the magnesium atoms form dimers, and substantially all of the magnesium has been replaced by scandium in the new phase. However, in this case the insertion of additional bridging atoms (Ga6 and Cu7) has made the Sc2−Sc2 distances too

(28) In terms of the numeric relationships, the title phase might be called a 1/0 − 2/1 − 1/0 AC in the jargon used for quasicrystals. The order of an AC is determined by its lattice parameters. Generally, the lattice parameters of quasicrystal (a_6) and its q/p cubic approximant crystal (AC) have a fixed mathematical relationship: $a_{q/p} = 2a_6(p+q\tau)/\sqrt{(2+\tau)}$, in which $\tau = 1.618$, the golden mean, and p and q are two consecutive Fibonacci numbers. Note that, however, zero is not a member of the Fibonacci series according to Fibonacci's original rabbit problem, yet it fits the mathematical expression of the problem: $F(n + 2) = F(n + 1) + F(n)$. Very few intermetallic phases have been referred to as 1/0 ACs.

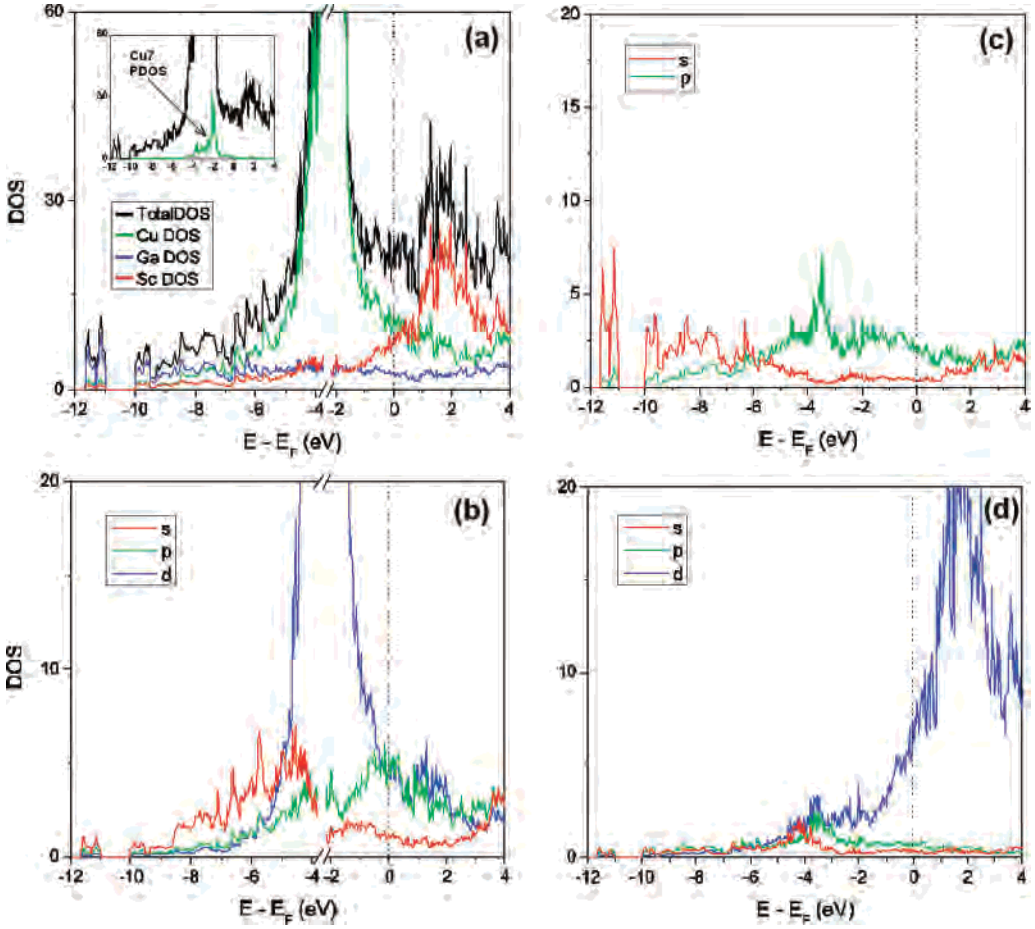

Figure 6. (a) Densities-of-states (DOS) per cell for hypothetical $Sc_4Cu_{15}Ga_7$. Inset: DOS of Cu7. The PDOS of (b) copper, (c) gallium, and (d) scandium are also shown. Note the break in the energy scale in (a) and (b).

large to be bonding (>7.0 Å), but Sc1−Sc1 and Sc3−Sc3 remain as dimers.

The 3D framework in part b of Figure 3 can be viewed as 2D layers interconnected by the bridging atoms along *b*. Part a of Figure 4 shows the projection of a single layer in which the repeat unit (circled) is $Cu_6@Cu_{8+8/2}Ga_{4/2}$. Each unit shares its Cu4−Cu4 and Ga3−Ga3 extremities with four like neighbors, and the Cu3−Cu3 edges, with both bridging atoms above and below the layer. In comparison with the green $Cu_6@Ga_{14}$ unit in $Mg_2Cu_6Ga_5$, the replacement of the gallium by copper in the Ga_{14} cage shrinks not only the cage but also the central Cu_6 octahedra (blue). As seen in part b of Figure 4, the latter have been squeezed along the *b* axis to give shorter apex (Cu6) to waist (Cu5 and Cu8) distances (∼2.53−2.65 Å) and elongated distances between waist atoms [*d*(Cu5−Cu8) = 3.05 Å]. Note that the Cu_6 octahedra in $Mg_2Cu_6Ga_5$ are regular, with all of the edge distances equal (2.633 Å).[8]

The zigzag chains of gallium-centered Cu_4Ga_6 arachno icosahedra, in part b of Figure 4, exhibit remarkable structure complexity and beauty. Note that the $Ga@Cu_{12}$ icosahedra in $Mg_2Cu_6Ga_5$ alternate with Mg−Mg dimers along the *c* direction.[8] In the new structure, the Cu_4Ga_6 arachno icosahedra form zigzag chains by sharing Ga5 atoms so that the respective Ga4 centers and the shared Ga5 atoms are lineally arranged (∠Ga4−Ga5−Ga4 = 179.98(3)°). (The Ga5 atoms are also collinear because they occur on the 4*f* (1/4, 1/4, 1/2) and equivalent sites.) Actually, the Sc1−Sc1 dimers also have suitable bonding distances to Cu1, Cu4, Ga1, and Ga5 (all <3.1 Å), such that they complete the former Cu_4Ga_6 arachno icosahedra to generate distorted heteratomic icosahedral chains. Simultaneously, the shared Ga5 atoms are also centers of heteratomic icosahedra defined by two Sc1−Sc1 dimers, four Cu1, two Ga1, and two Ga4 atoms. Therefore, the contents in large tunnels in effect consist of a highly condensed zigzag heteratomic icosahedral chain of a type never seen before.

Last, we consider the bridging Cu7 and Ga6 atoms, part c of Figure 4. According to the average structural data, the mean Cu7−Ga6 distances are ∼2.09 Å and for the Ga6−Cu3, ∼2.15 Å. The improbable shortness of these idealized bonds is solved in the present structure by the necessity that mixed Cu7/Mg and fractional Ga6 atoms never locate at these mean positions. Rather, both show incommensurate displacements, particularly large for Ga6. In addition, both of their occupancies become partial in the ternary structure when all of the magnesium is removed.

Part a of Figure 5 shows the modulated Cu7−Ga6 (red) and Cu3−Ga6 (blue) bond distance correlations in terms of the internal t coordinates, which are the projections of x4 onto the A_4 axis along R_3 direction in $(3+1)D$ space.[22] Both bond distances become reasonable through the saw-tooth-

like modulations (including both position and occupancy modulations). The modulations result mainly from the positional displacements in *dx* direction, as shown in part b of Figure 5, consistent with the observed electron densities (Figure 1) and the refined ADPs for the mean structure (Table S1 in the Supporting Information).

Some chemical aspects of the structural and electronic changes that relate the two phases are informative. The process with the parent as $2Mg_2Cu_6Ga_5 = Mg_4Cu_{12}Ga_{10}$ and yields the ternary $Sc_4Cu_{14.75}Ga_{7.5}$, during which all of the magnesium is first replaced by scandium with a gain of 4 e^-. At the same time, 2.5 galliums are removed and 2.75 coppers ($3d^{10}$ naturally) are added, which correspond to an overall change of $-2.5(3) + 2.75 = -4.75$ e^-. In other words, a net oxidation of only about 0.75 e^- per formula unit (~26 atoms) of product occurs during this transformation. (The equivalent calculation for the refined quaternary product gives a 0.33 e^- oxidation.) The distinctive structural functionalities of copper versus gallium appear to be most responsible for the changes seen in Figure 3. The cation features appear rather similar in both, and the major changes take place in gallium versus copper placements and functions. Green gallium is seen to be the principal framework generator in $Mg_2Cu_6Ga_5$ (left) with copper (blue) forming both the blue octahedra and the green icosahedra. The switch of some gallium to copper with the change in formulas (above) accompanies substantial alterations of atom roles as well as the cubic to orthorhombic distortion. The framework now becomes predominately copper, with only a little gallium left in the bridges around the outside. The octahedra remain copper but become appreciably distorted because the surrounding atoms are now mostly copper atoms, which form shorter bonds. A major change occurs in the former isolated gallium icosahedra, which are converted to condensed arachno icosahedral chains (green) with a Cu_4Ga_6 composition. As a result, Ga6 and Cu7 (circled) are inserted into the outer network in an incommensurate manner to avoid otherwise close contacts, presumably in a drive to fill space well and perhaps for bonding reasons (below).

Electronic Structure. Parts a–d of Figure 6 show the densities-of-states (DOS) and partial DOS (PDOS) of the hypothetical $Sc_4Cu_{15}Ga_7$ after necessary approximations regarding mixed and fractional sites. A total of 198 electrons per formula unit fill states up to the Fermi energy (E_F), which corresponds to $e/a = 1.85$ (without counting Cu $3d^{10}$ electrons). The value is close to the experimental e/a values of the title compositions (1.88–1.89). The DOS bands exhibit several general features similar to those of the $Sc_3Mg_{0.4}Cu_{10.5}Ga_{7.3}$ 1/1 AC and/or $Mg_2Cu_6Ga_5$.[8,9] As can be seen, the very broad copper 3d bands lie mainly ~2.0 eV below the E_F, but retain considerable contributions at E_F, in parts a and b of Figure 6, mainly through orbital mixings with scandium 3d and gallium 4p states. As for the scandium 3d states, they lie mainly ~2 eV above E_F, but they also contribute some states at E_F, more so than gallium 4p, as shown in parts c and d of Figure 6. Such a function is of course not provided by magnesium.

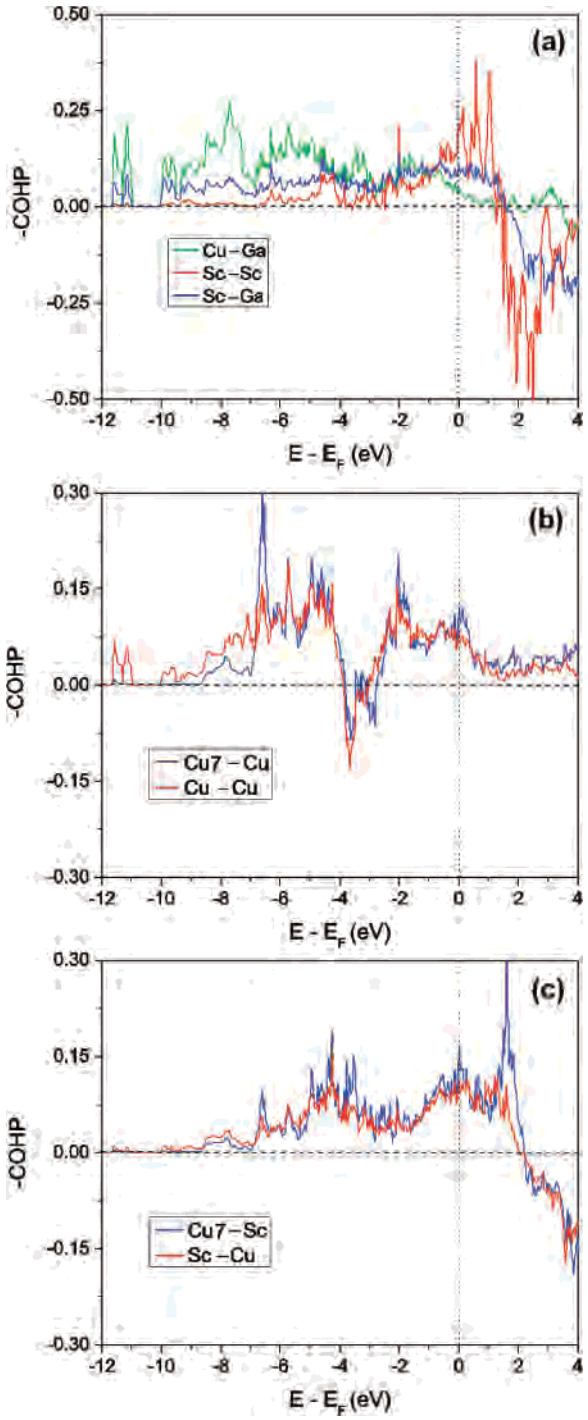

Figure 7. The crystal orbital hamilton population (–COHP) data (eV/bond) for (a) Cu–Ga, Sc–Sc, and Sc–Ga; (b) Cu7–Cu and Cu–Cu; and (c) Cu7–Sc and Cu–Sc in the hypothetical $Sc_4Cu_{15}Ga_7$. The bonds to Cu7 (Cu7–Cu and Cu7–Sc) exhibit considerable larger –COHP values at and above the Fermi energy than the average of corresponding types, suggesting that the Fermi surface is sensitive to the behavior of Cu7.

The crystal orbital hamilton population (COHP) data, in parts a–c of Figure 7, show that no bond type is fully optimized at E_F, suggesting that additional electrons might stabilize the structure. This may be another driving force for the inclusion of Ga6 in the title phase, although, unfortunately the diffuse and fractional Ga6 had to be excluded in the band calculations. We may alternatively consider Cu7, another atom that is strongly incommensurate,

to judge the importance of these bridging atoms in bonding and, eventually, a possible reason for the incommensurate modulations. As shown in the inset of part a of Figure 7, the PDOS for all of the Cu7 orbitals lies between −2.3 and − 1.6 eV, on the right side of the large copper 3d band. Therefore, the Fermi surface properties should be rather more sensitive to Cu7 than to the other copper atoms, suggesting the bridging atoms (or the incommensurate modulations generated by them) play important roles in this structure. The comparisons of −COHP data between Cu7−Cu versus all of the Cu−Cu and Cu7−Sc versus all of the Cu−Sc also support this idea. In parts b and c of Figure 7, the −COHP contributions of Cu7 to bonding are seen to be larger than the average of both Cu−Cu and Sc−Cu bonds, especially at E_F and up to ∼1.5 eV higher.

Conclusions

The newly synthesized, incommensurately modulated $Sc_4Mg_xCu_{15-x}Ga_{\sim 7.5}$ solid solution (refined for $x = \sim 0, 0.5$) has close relationships not only to its parent, $Mg_2Cu_6Ga_5$,[8] but also to Sc−Mg−Cu−Ga 1/1 AC and QC.[9] Therefore, this phase offers a bridge of sorts between the Mg_2Zn_{11}-type phases, the precursors, and the AC and QC phases gained by means of pseudogap electronic tuning. The term 1/0−2/1−1/0 AC for the title phase[28] best identifies this idea because icosahedral QCs (*i*-QCs) can be considered as a type of 3D, incommensurately modulated crystals. We believe that the attainment of additional crystals with 1D or 2D incommensurate modulations might help considerably in cracking the secret structures of *i*-QCs. Although the average structure gained provides the general features for the title phase, some cautions regarding the superspace refinements remain because of the limited incommensurate reflection intensities.

Acknowledgment. We thank Prof. V. Petříček for his kind help with and education on incommensurate structure refinements with JANA2006. This research was supported by the U.S. National Science Foundation, Solid-State Chemistry, via grant DMR-0444657 and was performed in the facilities of the Ames Laboratory, U.S. Department of Energy.

Supporting Information Available: Figures, tables, and CIF data for the two standard and the incommensurate refinements. This material is available free of charge via the Internet at http://pubs.acs.org.

IC701853C